Supporting Information

Self-Assembly Processes of 2D Au(I)-S$(CH_2)_2$COOH Lamellae

Shengrui Zhang[a], Zhongqi Yu[a], Aude Demessence[b,*], Nathalie Guillou[c], Shujue Xu[a], Han Liu[a], Yuru Fu[a], Jingpei Zhang[a], Minjie Li[a,*]

[a] State Key Lab of Supramolecular Structure and Materials, College of Chemistry, Jilin University, Changchun, 130012, P. R. China.

E-mail: liminjie@jlu.edu.cn

[b] Univ Lyon, Université Claude Bernard Lyon 1, CNRS, Institut de recherches sur la catalyse et l'environnement de Lyon (IRCELYON), Villeurbanne, France.

E-mail: aude.demessence@ircelyon.univ-lyon1.fr

[c] Université Paris-Saclay, UVSQ, CNRS, UMR 8180, Institut Lavoisier de Versailles, 78000, Versailles, France.

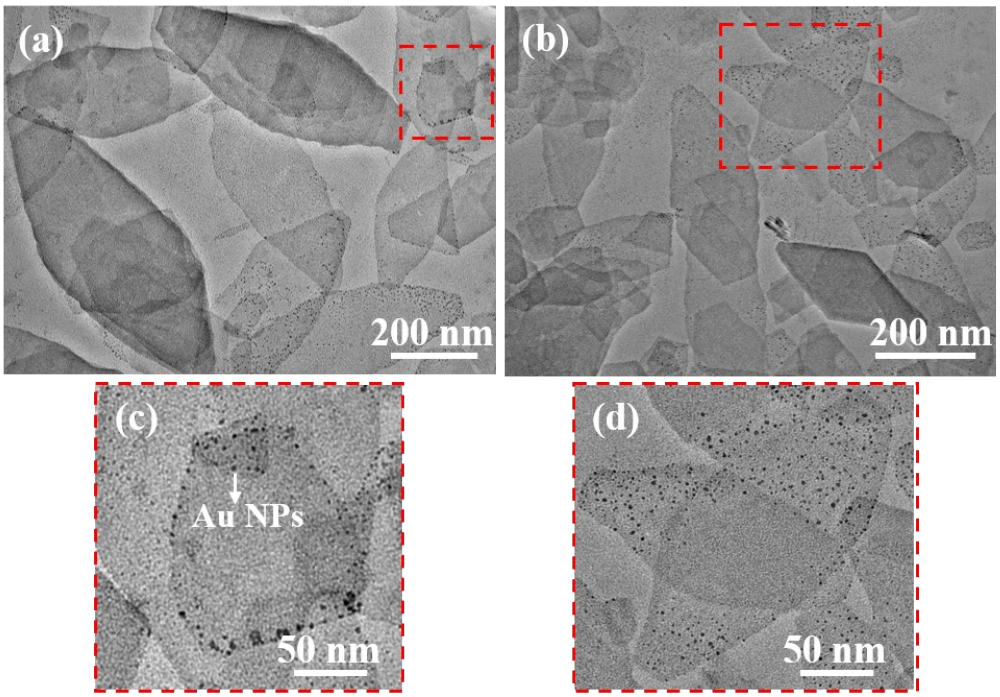

Figure S1. TEM images of Au(I)-MPA-water. The edges (c) and thinner locations (d) of the 2D lamellae first become gold nanoparticles after being bombarded with electron beams.

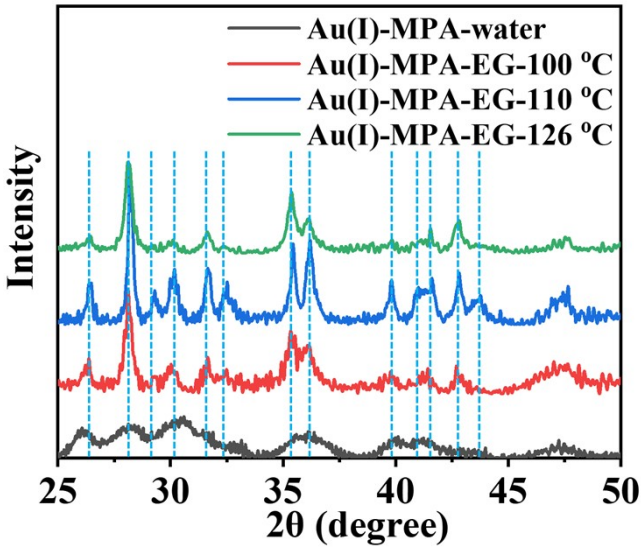

Figure S2. PXRD patterns (25° ~ 50°) of Au(I)-MPA-water and Au(I)-MPA-EG-100/110/126 °C.

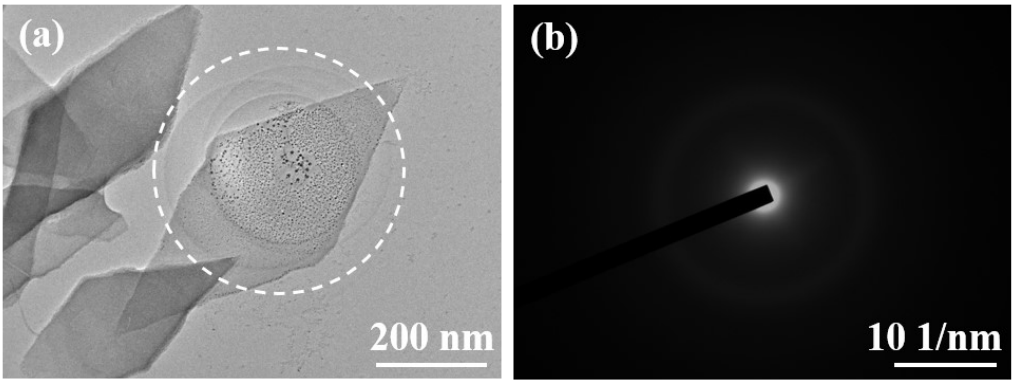

Figure S3. TEM image (a) and SAED pattern (b) of Au(I)-MPA-EG-110 ^{o}C under ordinary TEM.

The white circle is the region under focused electron beam, where the 2D lamellae decompose into gold nanoparticles.

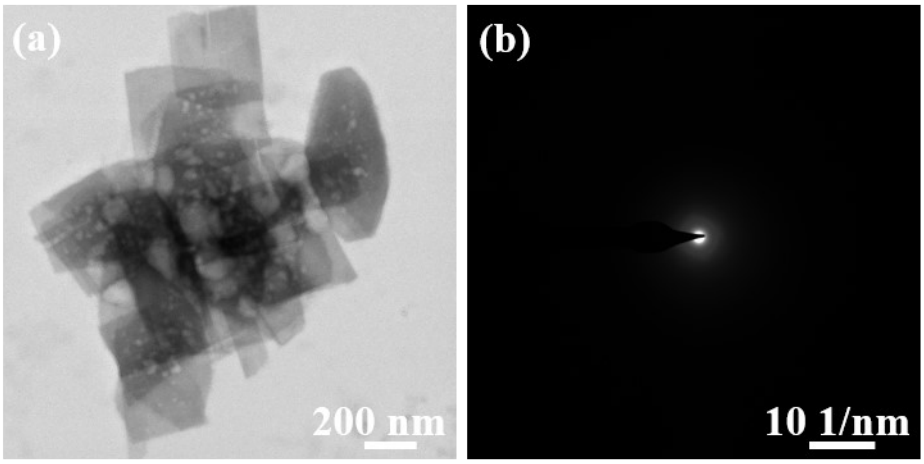

Figure S4. Cryo-TEM image (a) and SAED pattern (b) of Au(I)-MPA-water.

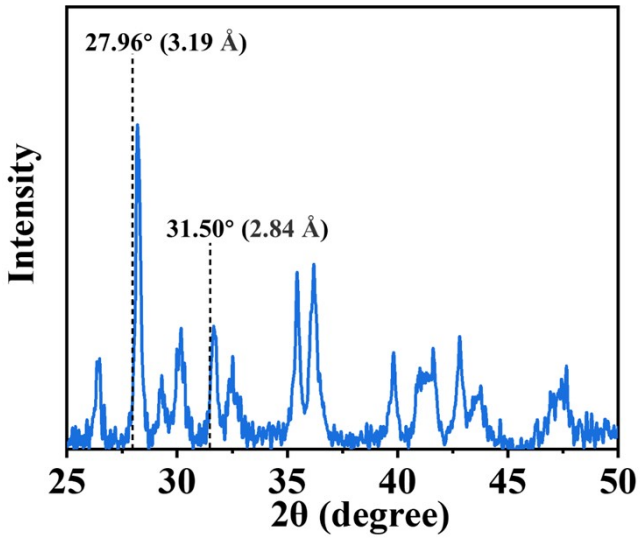

Figure S5. Inter-plane spacings in SAED found in PXRD patterns of Au(I)-MPA-EG-110 ^{o}C.

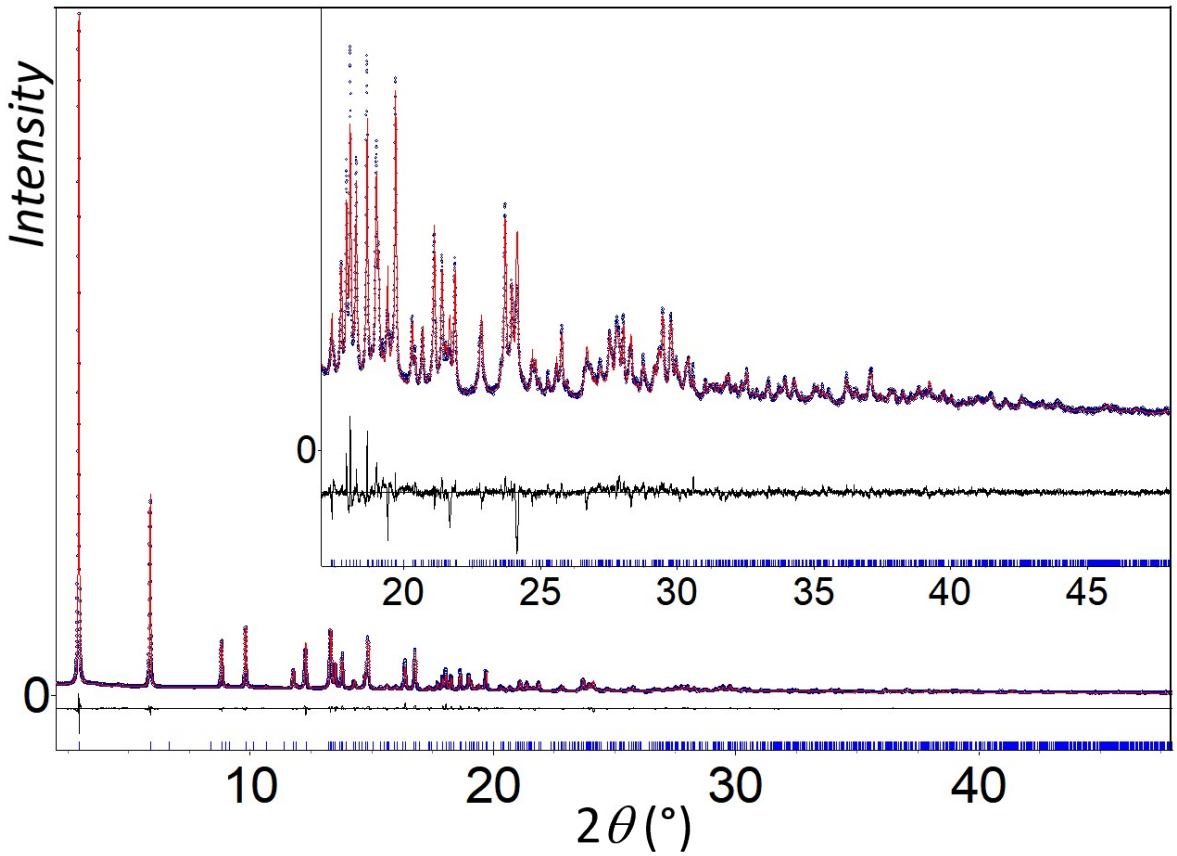

Figure S6. Final Rietveld plot of 2D Ag(I)-MPA lamellae showing observed (blue circles), calculated (red line), and difference (black line) curves.

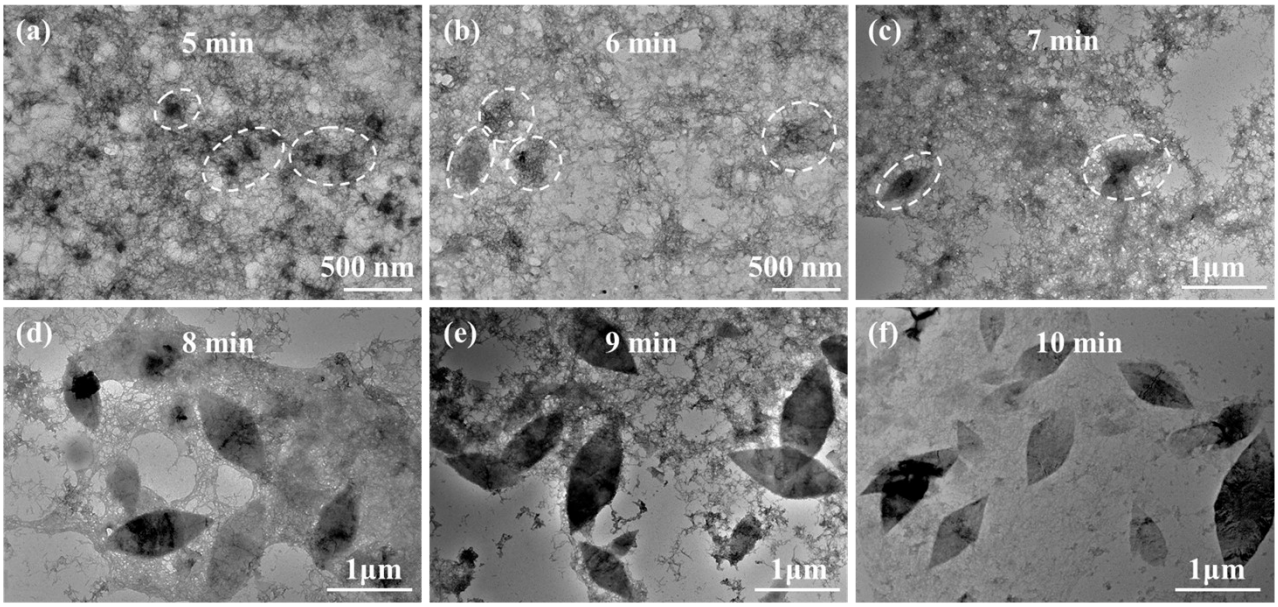

Figure S7. TEM monitoring of the assembly of Au(I)-MPA-EG-110 °C with time. Different from the assembly of Au(I)-MPA-EG-126 °C, in which irregular 2D lamellae are clearly observed during the early stage, the assembly and crystallization of Au(I)-MPA-EG-110 °C does not show clear 2D lamellae but blurred aggregates (5 and 6 min, indicated with white circles) of the 1D pre-assemblies, once 2D lamellae can be observed (7 min, indicated with white circles), they are already in olive shape, and then their size increases with time without a clear re-shaping processes (7 - 10 min).

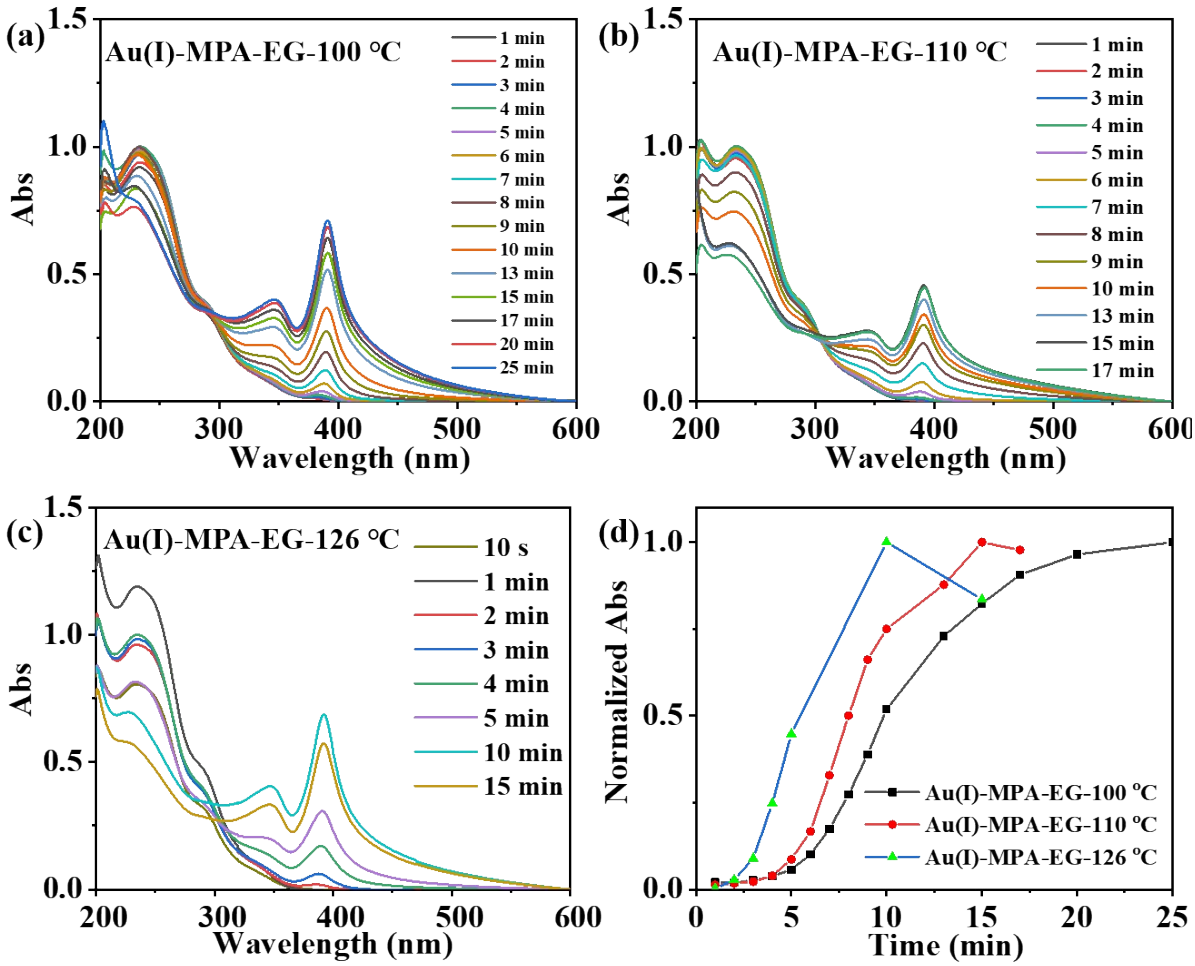

Figure S8. (a, b, c) UV-vis spectral monitoring the assembly of Au(I)-MPA-EG-100/110/126 °C ([Au] = 1.00 × 10^{-4} M in UV-vis spectra). (d) Changes of Abs at peak absorption around 392 nm of Au(I)-MPA-EG-100/110/126 °C. The final drop of absorption of Au(I)-MPA-EG-110 and 126 °C is due to the precipitation of the products.

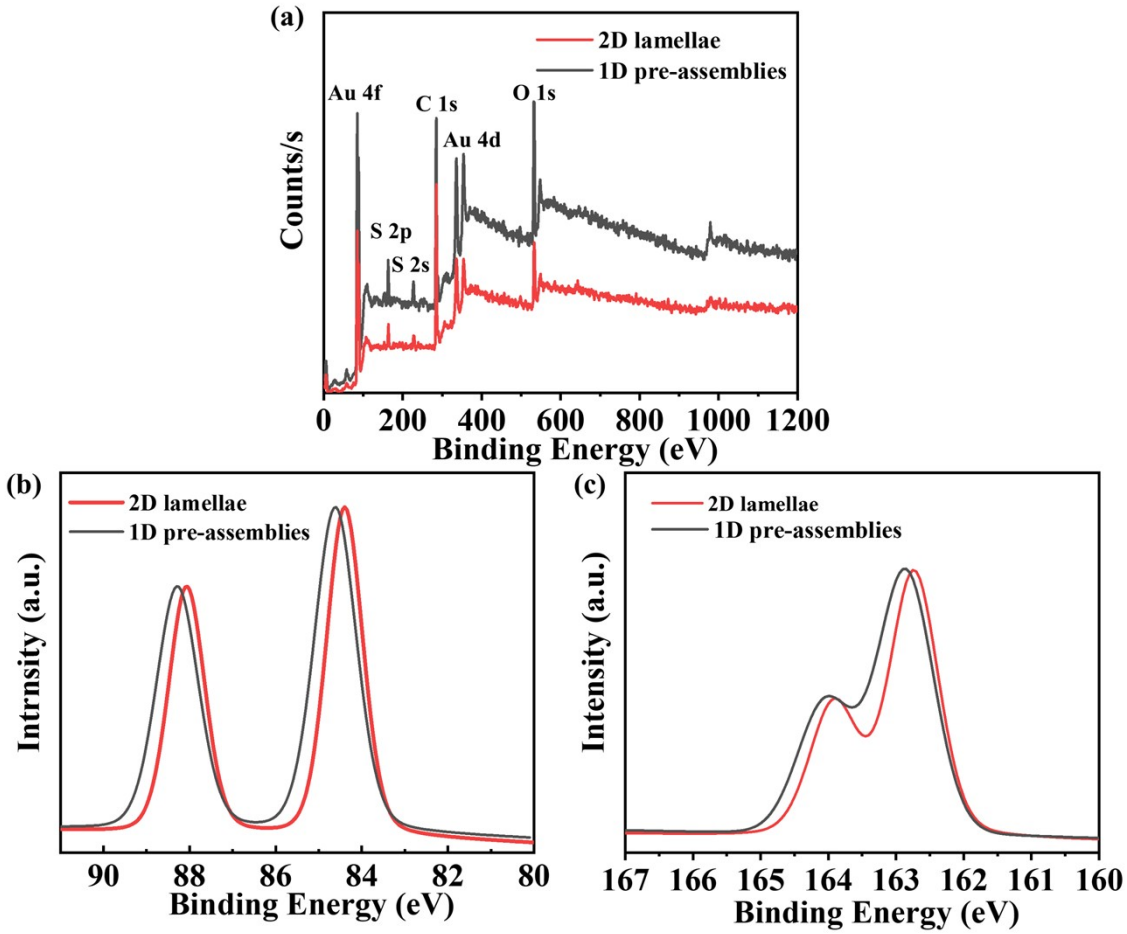

Figure S9. (a) XPS surveys of 2D Au(I)-MPA lamellae and 1D pre-assemblies. which show the same Au, S, C and O elements in the assemblies. High-resolution XPS of 2D lamellae and 1D pre-assemblies with (a) Au, (b) S elements.

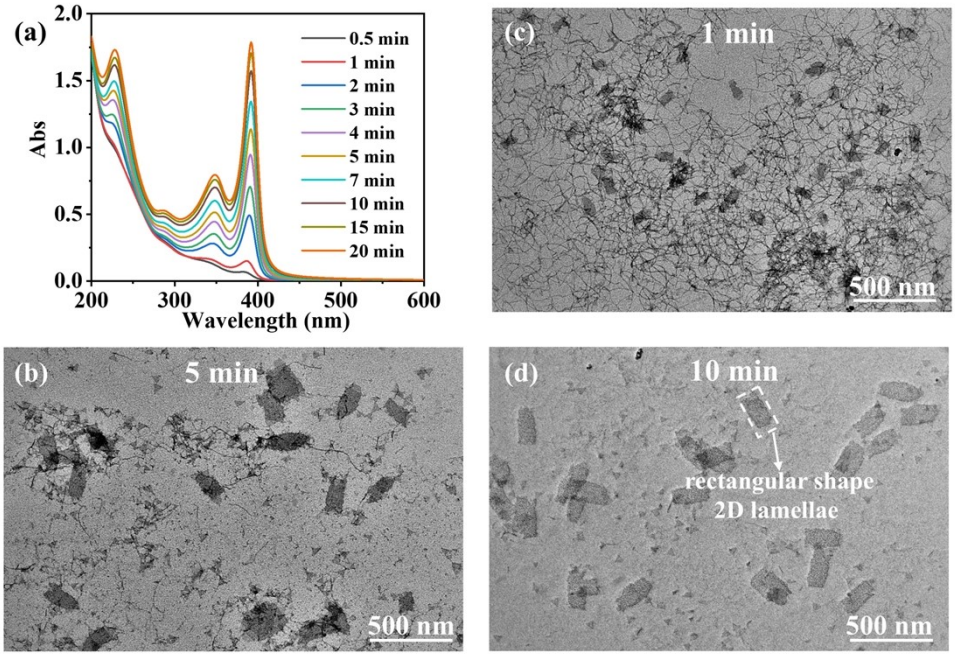

Figure S10. (a) UV-vis spectral monitoring the of Au(I)-MPA-water ([Au] = 1.00×10^{-4} M in UV-vis spectra). TEM images of Au(I)-MPA-water assembled at (b) 1 min, (c) 5 min, and (d) 10 min.

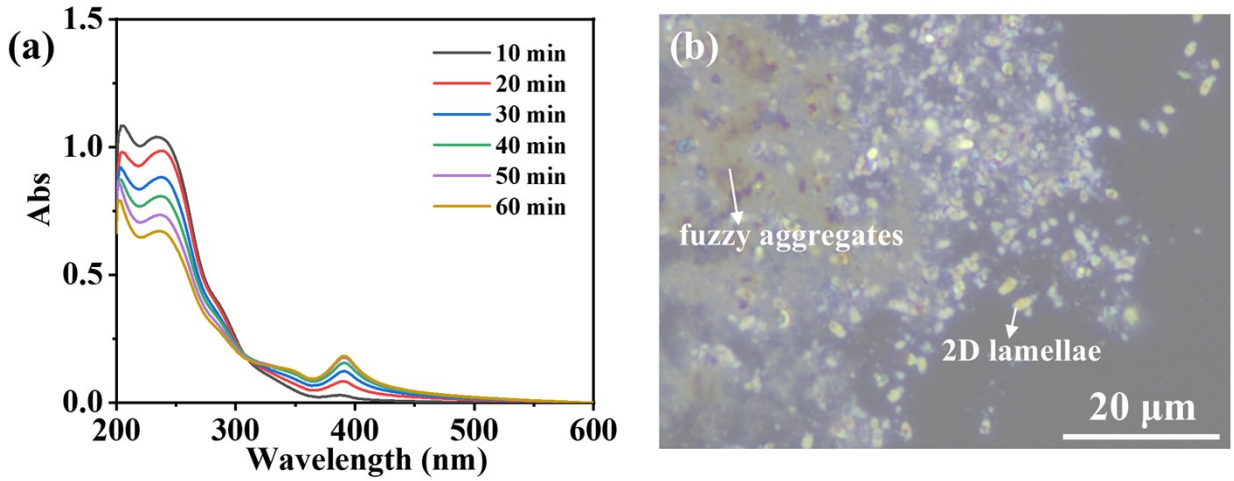

Figure S11. (a) UV-vis absorption spectral monitoring of the assembly of Au(I)-MPA-EG (water content = 1.78%) at 100 °C ([Au] = 1.00 × 10^{-4} M in UV-vis spectra) and the corresponding (b) optical microscopy image of the final products at 60 min. In addition to 2D lamellae, fuzzy aggregates are observed which are probably formed by the large amount of remaining 1D pre-assemblies.

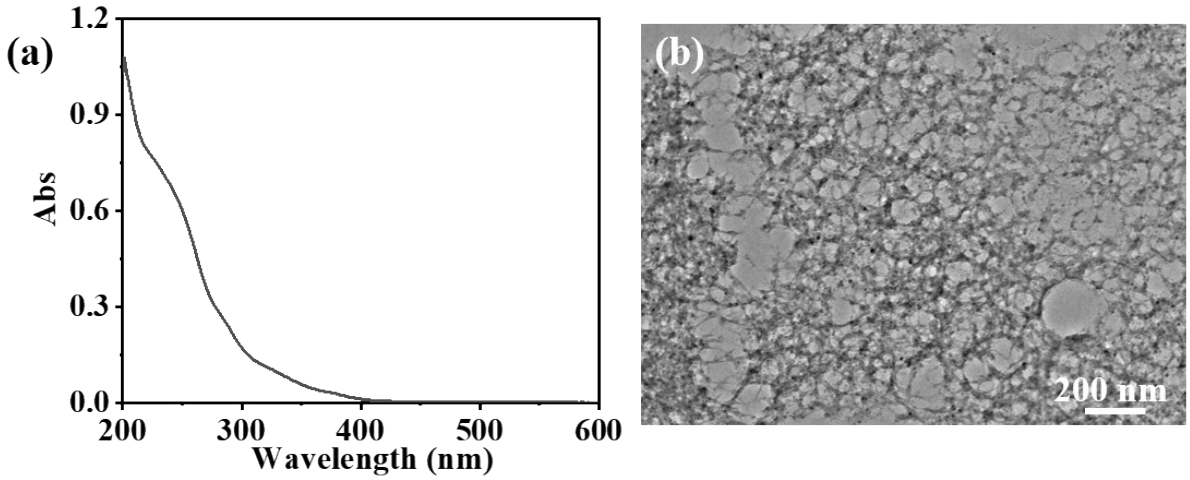

Figure S12. UV-vis absorption spectrum (a) and TEM image (b) of Au(I)-MPA-EG assemblies (water content = 1.78%) prepared at 176 °C for 60 min ([Au] = 1.00×10^{-4} M in UV-vis spectra).

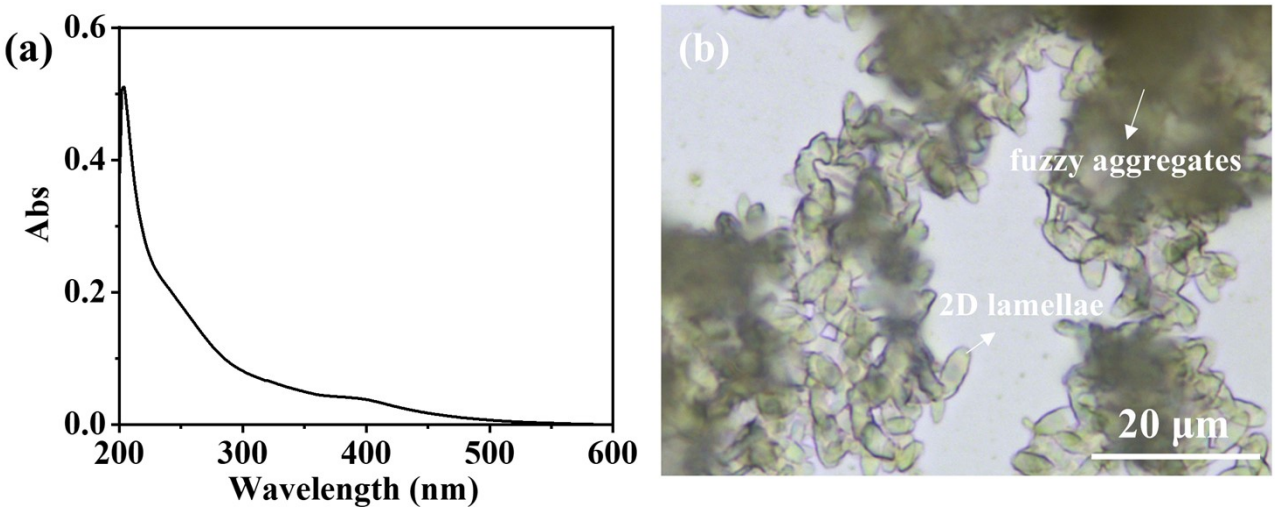

Figure S13. UV-vis absorption spectrum (a) and optical microscopy image (b) of Au(I)-MPA-EG (water content = 1.78%) at 60 min ([Au] = 1.00×10^{-4} M in UV-vis spectra). In addition to 2D lamellae, fuzzy aggregates are observed which are probably formed by the large amount of remaining 1D pre-assemblies.

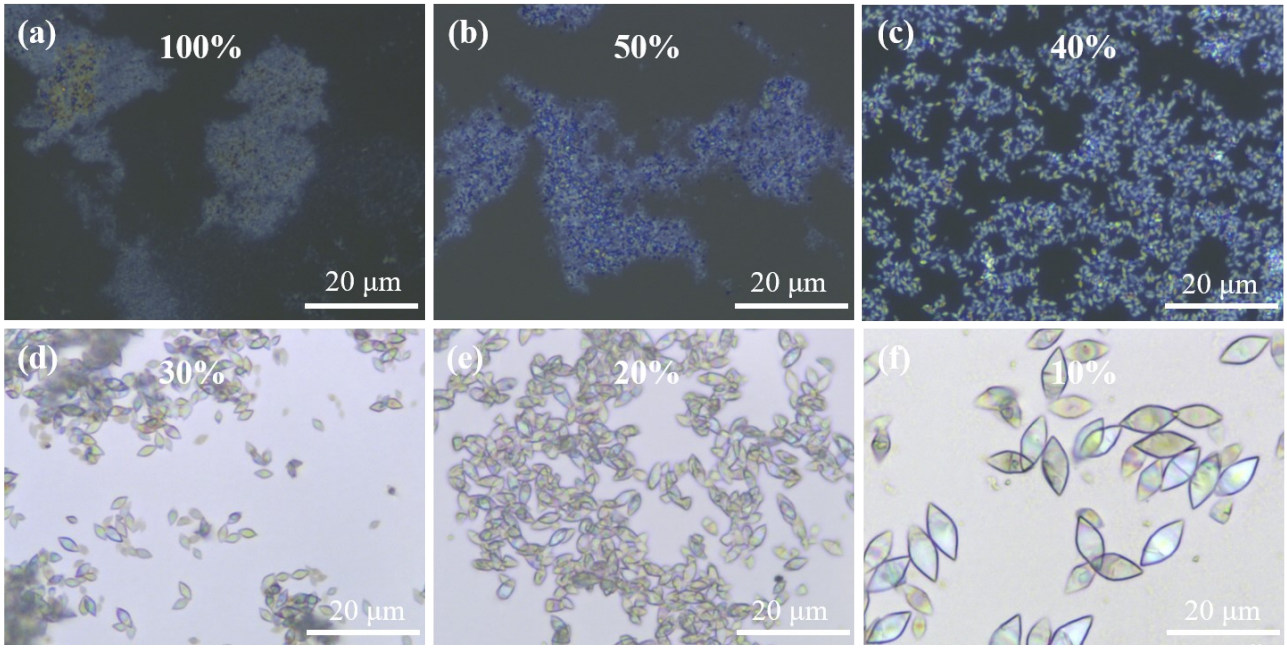

Figure S14. Optical microscopy images of 2D Au(I)-MPA lamellae prepared with different water contents. (a) 100%, (b) 50%, (c) 40%, (d) 30%, (e) 20%, (f) 10%. Due to low-resolution of optical microscope, 2D Au(I)-MPA lamellae prepared with 100% and 50% water cannot be clearly seen.

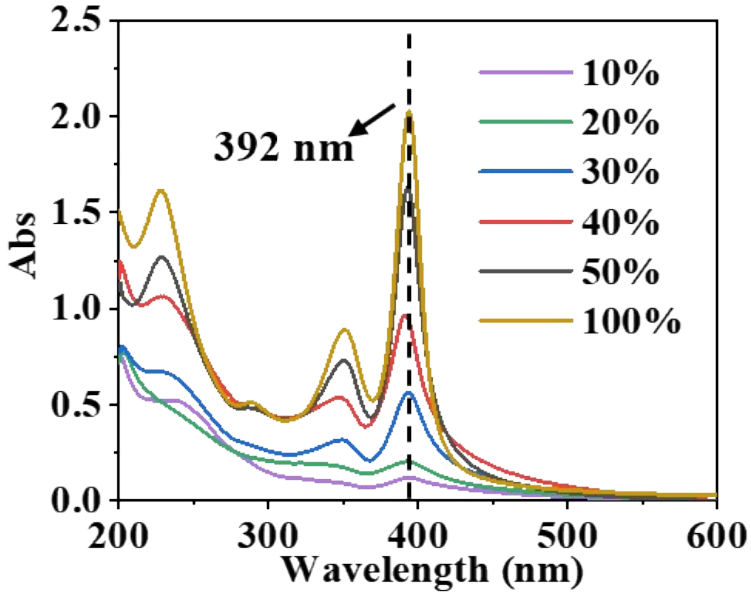

Figure S15. UV-vis spectra of 2D Au(I)-MPA lamellae prepared with different water contents ([Au] = 1.00×10^{-4} M in UV-vis spectra).

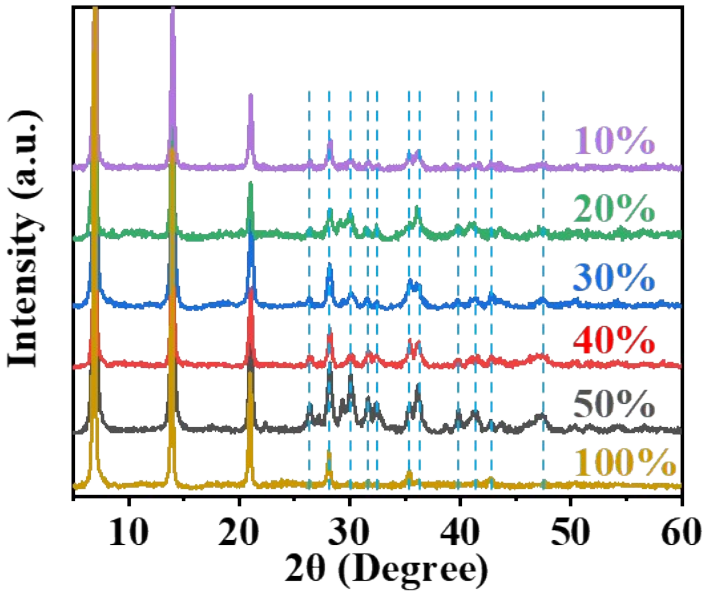

Figure S16. PXRD patterns of 2D Au(I)-MPA lamellae prepared with different water contents.

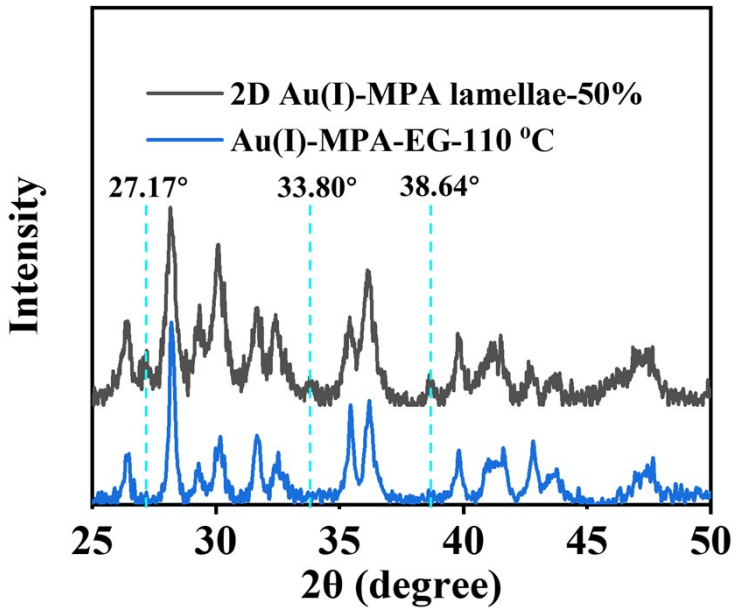

Figure S17. PXRD patterns (25° ~ 50°) of 2D Au(I)-MPA lamellae prepared at 50% water content and Au(I)-MPA-EG-110 °C.

Table S1. Crystallographic data and Rietveld refinement parameters for 2D Ag(I)-MPA lamellae.

	$[Ag(SC_2H_4CO_2H)]_n$
Empirical formula	$C_3H_5Ag_1O_2S_1$
M_r	213.00
Crystal system	monoclinic
Space group	$P2_1/c$
a (Å)	13.6120(2)
b (Å)	6.63372(6)
c (Å)	5.94002(5)
β (°)	99.695(1)
V (Å^3)	528.71(1)
M_{20}	64
Z	4
λ (Å)	0.6887
No. struct. parameters	24
No. of reflections	940
R_p, R_{wp}	0.034, 0.047
R_{Bragg}, GoF	0.016, 2.90

Table S2. XPS analyses of Au(I)-MPA-water 2D lamellae and 1D pre-assemblies.

	2D lamellae	**1D pre-assemblies**
Binding Energy of Au $4f_{7/2}$	84.45 eV	84.64 eV
FWHM of Au $4f_{7/2}$	0.94 eV	1.13 eV
Binding Energy of S $2p_{3/2}$	162.73 eV	162.86 eV
FWHM of S $2p_{3/2}$	0.88 eV	0.92 eV